Teleported CNOT Gate between GKP Qubit States: Final Report

Francisco Estrella
Supervisor: Prof. Shyam Shankar (Department of Electrical Engineering)

December 15, 2021

Abstract

It has been demonstrated that a deterministic quantum gate teleportation circuit for a CNOT gate can be efficiently implemented using logical qubits encoded in oscillators of superconducting quantum circuits structured in a modular architecture[1]. The main encoding used to define the logical qubits consisted of the first-level bosonic binomial quantum code; a code that can correct for errors due to photon loss, which is typical in this type of hardware. A similar encoding that has been proposed in other quantum computing platforms based on oscillators consists of Gottesman-Kitaev-Preskill (GKP) states. GKP states also allow for the detection of photon loss as well as other common types of errors. The objective of this project is to investigate the efficiency of the quantum gate teleportation circuit with qubit encodings based on GKP states to produce an effective CNOT gate.

The approach taken to address this problem consists of constructing an analog version of the quantum gate teleportation circuit for continuous variable (CV) states, the category of states that include GKP states. Xanadu's quantum computing software library[2] contains modules that can be used to simulate CV quantum circuits. The CV version of the quantum gate teleportation circuit was simulated using this library. The efficiency was tested using fidelity operations.

GKP states are a promising tool for fault-tolerant quantum computation in models based on oscillators. By simulating the gate teleported circuit with GKP states, it will become clearer what experimental factors are needed to bring this circuit into reality using a modular quantum computing architecture.

1 Introduction

This report is divided into 6 main sections. The first is the Theoretical Background where the continuous variable picture of quantum computing is introduced. Here, GKP states are also defined. The second is Experimental Background where the experiment of interest ins introduced and the main objective of the project is described. The third part is Simulation Background. This is where the particular circuit simulated is introduced and a more specific task that would solve the main objective is described. The next section, Numerical Simulations, shows the results of the simulations done to solve the main objective. Here, a major setback is also presented. Next is Further Directions where relevant tasks that were not done in this project are outline as improvements of this study. Lastly, the section Skills Learned describes a few major skills developed throughout the time of work in this project.

2 Theoretical Background

2.1 Quantum Harmonic Oscillator

The quantum harmonic oscillator (QHO) is the quantum version of a classical harmonic oscillator. The latter being a simple pendulum or a simple spring, for example. The QHO can be described by the Hamiltonians

$$\begin{aligned} \hat{H} &= \frac{\hat{p}^2}{2m} + \frac{1}{2}m\omega^2\hat{x}^2 \\ \hat{H} &= \hbar\omega(\hat{a}^\dagger\hat{a} + \frac{1}{2}), \end{aligned} \tag{1}$$

where $\hat{p}$ and $\hat{x}$ are the momentum and position operators, respectively; $\hbar$ denotes the reduced Planck's constant, m is the mass of the oscillator, and ω represents the angular frequency of the oscillator. The first Hamiltonian represents the QHO state in position space or momentum space. In the second Hamiltonian, the operator $\hat{a}$ and its complex-conjugated form $\hat{a}^\dagger$ are used such that the QHO energy states can be expressed by levels as $|n\rangle$. Here, n physically represents the number of particles in that state. As an example, the state $|0\rangle$ represents a state with no particles; while the state $|50\rangle$ represents a state with 50 particles. This representation of a QHO state is called the number representation or Fock basis. In this basis the operator $\hat{a}$ and $\hat{a}^\dagger$ act as follows

$$\begin{aligned} \hat{a}^\dagger |n\rangle &= \sqrt{n+1}\,|n+1\rangle \\ \hat{a}\,|n\rangle &= \sqrt{n}\,|n-1\rangle\,. \end{aligned} \tag{2}$$

From these expressions, it is clear why the operators $\hat{a}$ and $\hat{a}^\dagger$ are usually called the raising and lowering operators. The number representation or Fock basis was introduced for reference. Another representation is of major importance for this study. This is the continuous variable representation. To introduce this

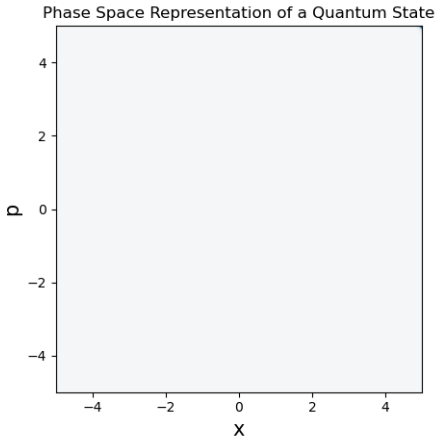

Figure 1: Phase Space Setting of Quantum Harmonic Oscillator State

picture, first notice that the position and momentum operators can be expressed in terms of the raising and lowering operators as follows

$$\begin{aligned} \hat{x} &= \sqrt{\frac{\hbar}{2m\omega}}(\hat{a}^\dagger + \hat{a}) \\ \hat{p} &= i\sqrt{\frac{\hbar m\omega}{2}}(\hat{a}^\dagger - \hat{a}). \end{aligned} \tag{3}$$

These operators have a continuous eigenvalue spectrum defined by $(-\infty, \infty)$. This is where the term "continuous variable" comes from. It is possible then to represent a QHO state as a distribution in a phase space defined by eigenvalues of these two observable operators. The phase space would look as in Fig 1., where the axes correspond to the eigenvalues of $\hat{x}$ (x-axis) and $\hat{p}$ (y-axis). In this picture, the operators $\hat{x}$ and $\hat{p}$ are also called quadrature operators.

2.2 Wigner Function

Just as a quantum state can be represented by a wave function or a density operator, there is an alternative description of a quantum state apart in the phase space picture. This description is given by a quasi-probability distribution in phase space known as a Wigner function. It is a quasi-probability distribution because it can be negatively valued at some points. The main idea is to keep in mind is that positive-valued distributions, either in position space or momentum space, can be obtained from the Wigner function.

2.3 Gaussian States

As an example, the Wigner distribution of the zero particle state in the Fock basis, $|0\rangle$, is shown in Fig. 2. This consists of a Gaussian distribution cen-

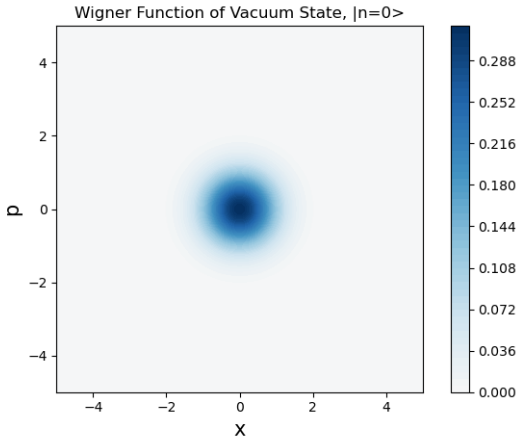

Figure 2: Wigner Function of the Vacuum State $|0\rangle$

tered at the origin of phase space with equal variances in all directions. Being a Gaussian distribution, it can be characterized by a vector of means, which gives information about the mean location of the distribution in phase space, and a covariance matrix, which gives information about the variances of the distribution. In this case, the $|0\rangle$ becomes a Gaussian state in the phase space picture; a state whose Wigner function is a Gaussian distribution. Another example of a Gaussian state is the coherent state $|\alpha\rangle$. This state is defined in the Fock basis by

$$\hat{a}\,|\alpha\rangle = \alpha\,|\alpha\rangle\,. \tag{4}$$

In other words, a coherent state is an eigenstate of the lowering operator with eigenvalue α; where $\alpha \in \mathbb{C}$. The real and imaginary parts of α give information about the mean location of the distribution corresponding to a coherent state. Fig. 3 shows the Wigner function of a coherent state defined by $\alpha = 1.0 + 1.0j$. The real part is linked to the mean x location and the imaginary part to the mean p location.

2.4 Quantum Information Processing with Continuous Variables

Now that two quantum states have been introduced in the continuous variable description, it is possible to ask if quantum information processing can be done with these states. A few operators that can act as quantum gates on these states will now be introduced. An important point to keep in mind is that these are not all quantum gates in the continuous variable picture; only the relevant gates of this study are shown.

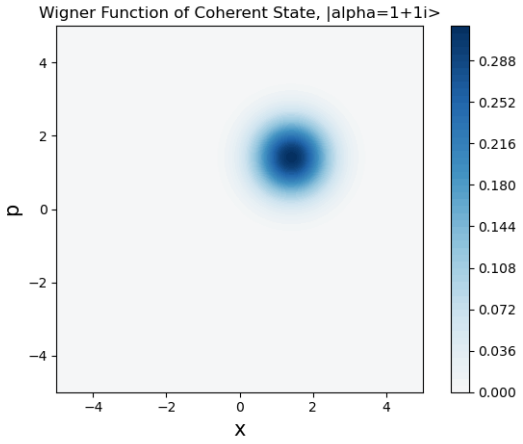

Figure 3: Wigner Function of a Coherent State $|\alpha = 1 + 1i\rangle$

2.4.1 Displacement Gate

The displacement gate $D(\alpha)$ is defined by the following action on the position and momentum operators

$$\begin{aligned} D^\dagger(\alpha)\hat{x}D(\alpha) &= \hat{x} + \sqrt{2\hbar}\mathrm{Re}(\alpha)\hat{\mathbf{1}} \\ D^\dagger(\alpha)\hat{p}D(\alpha) &= \hat{p} + \sqrt{2\hbar}\mathrm{Im}(\alpha)\hat{\mathbf{1}}. \end{aligned} \tag{5}$$

Here, the parameter α is complex-valued and determines the change in the vector of means of the quantum state. The covariance matrix is not modified under this gate. Note that a coherent state can be thought of as a displacement gate acting on the vacuum state.

2.4.2 Squeezing Gate

The squeezing gate $S(r)$ is defined by the following action on the position and momentum operators

$$\begin{aligned} S^\dagger(r)\hat{x}S^\dagger(r) &= e^{-r}\hat{x} \\ S^\dagger(r)\hat{p}S^\dagger(r) &= e^{r}\hat{p}. \end{aligned} \tag{6}$$

The parameter r is real valued and determines the amount of 'squeezing'. Squeezing refers to the reduction or amplification of the variance, whether that refers to the variance in $\hat{x}$ or $\hat{p}$. For example, if $r > 0$, then the variance in $\hat{x}$ will be reduced while the variance in $\hat{p}$ will be extended. Fig. 4 shows the Wigner function of a vacuum state acted upon by a squeezing gate with parameter $r = 0.5$.

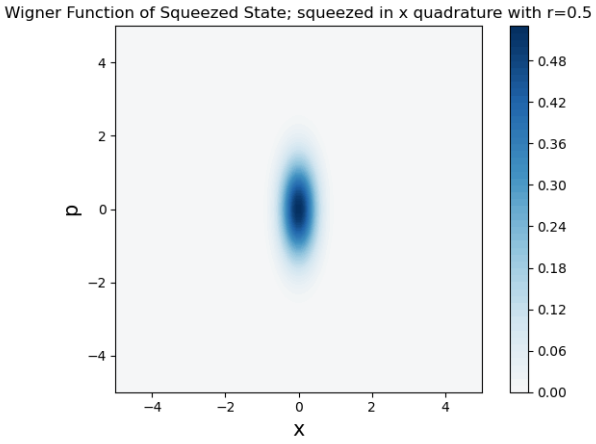

Figure 4: Squeezed vacuum state with a squeezing parameter of $r = 0.5$

2.4.3 Two-Mode Squeezing gate

The two-mode squeezing gate does not squeeze the quadrature operators of two modes as the name might suggest, rather, it squeezes linear combinations of the quadrature operators as follows

$$\begin{aligned} \hat{x}_1(t) \pm \hat{x}_2(t) &= (\hat{x}_1(0) \pm \hat{x}_2(0))e^{\pm r} \\ \hat{p}_1(t) \pm \hat{p}_2(t) &= (\hat{p}_1(0) \pm \hat{x}_2(0))e^{\mp r}, \end{aligned} \tag{7}$$

where r denotes the two-mode squeezing gate parameter. The left hand side of both equations denotes the operators after the action of a two-mode squeezing gate, and the terms inside parenthesis on the right hand side denote linear combinations of the operators before the action of the gate.

This gate is relevant because it creates entanglement between the two modes. Fig 5 shows plots of wave functions with common quadrature operators as the axes before the action of a two-mode squeezing gate (top figures) and after the action of a two-mode squeezing gate (bottom figures). Notice that after the application of the gate, the position observables have become correlated while the momentum observables have become anticorrelated. In the limit of $r \to \infty$, there is perfect correlation and anticorrelation.

2.4.4 Homodyne measurement

Homodyne measurements measure either the quadrature operator $\hat{x}$ or $\hat{p}$ of a mode. The probability distributions for these measurements can be obtained from the Wigner function as pointed out earlier.

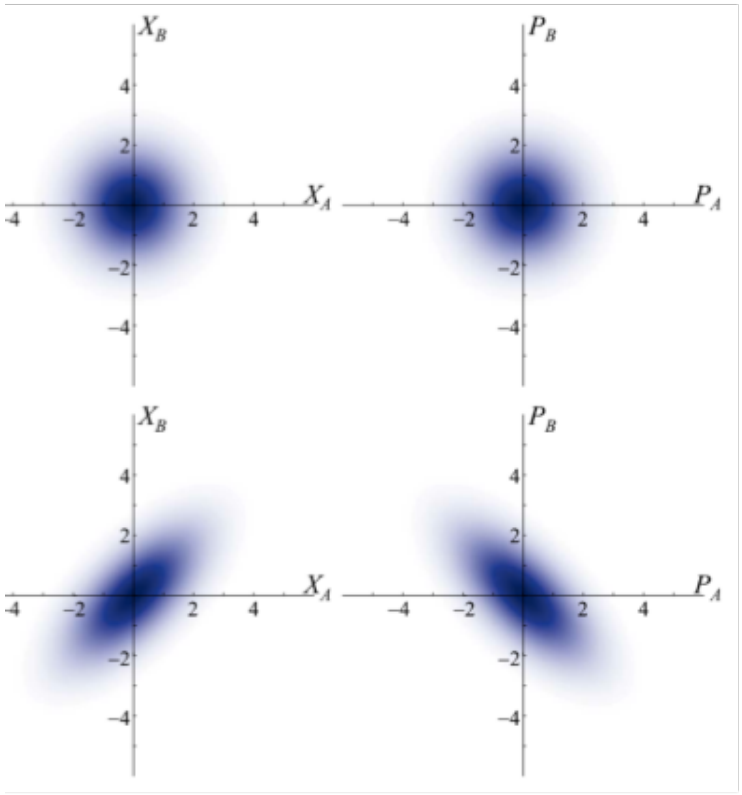

Figure 5: Wave functions of two vacuum modes before (top figures) and after (bottom figures) the application of a two-mode squeezing gate. Image taken from reference 4.

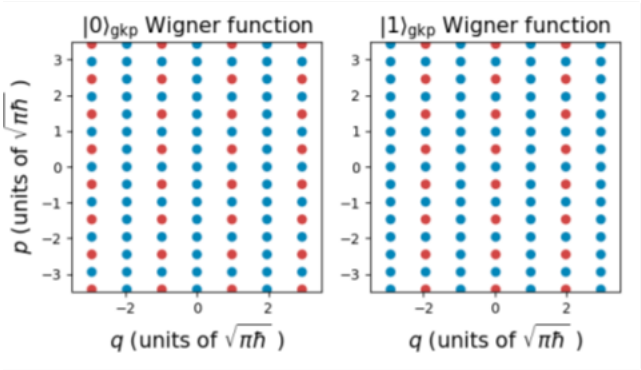

Figure 6: Ideal GKP states. Left figure shows the state $|0\rangle_{GKP}$. Right figure shows the state $|1\rangle_{GKP}$. Image taken from reference 2.

2.5 Non-Gaussian States: GKP States

Non-Gaussian states are those whose Wigner function is not Gaussian but could be a linear-combination of Gaussians. A particular example of these states are GKP (Gottesman-Kitaev-Preskill) states. In their ideal form, these states can be thought of as infinite lattices of delta functions in phase space. Fig. 6 shows two example of ideal GKP states. Each blue dot represents a delta function with a positive weight, while each red dot represents a delta function with a negative weight. These particular patterns can be used to define the qubit states $|0\rangle_{GKP}$ and $|1\rangle_{GKP}$ such that an arbitrary GKP state can be expressed as a linear combination of these two as follows

$$|\psi\rangle_{GKP} = \cos\frac{\theta}{2}|0\rangle_{GKP} + e^{-i}\sin\frac{\theta}{2}|1\rangle_{GKP} \tag{8}$$

In practice, ideal GKP states cannot be generated since they would require an infinite amount of energy. This leads to the definition of finite-energy GKP states. These are obtained by applying a damping operator on the ideal GKP states as follows

$$|\psi_\epsilon\rangle \equiv E(\epsilon)|\psi_I\rangle \qquad , E(\epsilon) \equiv e^{-\epsilon\hat{n}} \tag{9}$$

, where $|\psi_I\rangle$ represents an ideal GKP state, $|\psi_\epsilon\rangle$ represents a finite-energy GKP state, $E(\epsilon)$ represents the damping operator that creates the finite-energy GKP state, and ϵ represents is the damping operator that will determine the form of the finite-energy GKP state.

Fig. 7 shows an example of a finite-energy GKP state. Notice that this state has acquired two widths. One of them (σ) determines the width of each Gaussian distribution which used to be a delta function in the ideal case. The second (Δ) determines the width of the Gaussian or 'envelope' covering the full lattice. In the ideal case, we had n infinite lattice; now we have a finite lattice whose size is

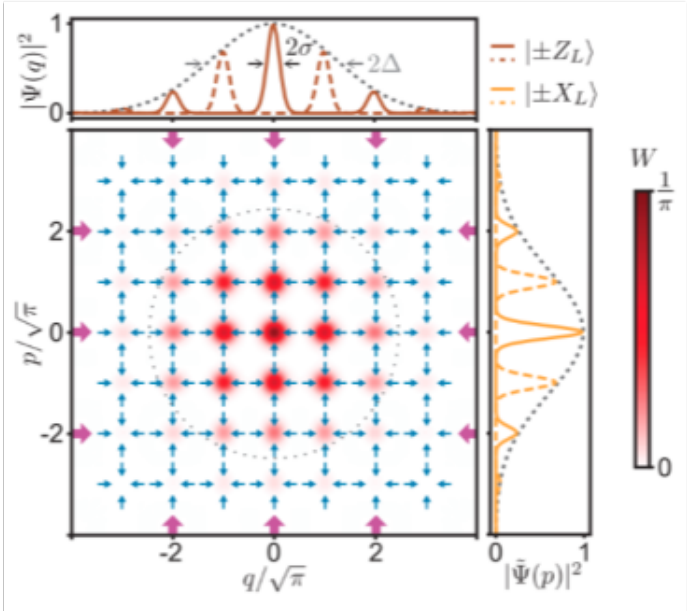

Figure 7: Finite-energy GKP state. Image taken from reference 4.

determined by Δ. The particular values of the widths σ and Δ of a finite-energy GKP state will be determined by the choice of the damping parameter ϵ. Fig. 8 shows finite-energy GKP states for different choices of the damping parameter ϵ. Notice that as the damping parameter increases, the width Δ decreases, while the width σ increases.

2.6 Universal Quantum Computation with Continuous Variables

We can now ask if universal quantum computation is available with continuous variables. Indeed, this has been proven. But it is important to point out that any quantum information processing task that cannot be simulated efficiently on a classical computer would require the use of non-Gaussian states, such as GKP states.

Even if the theory allows for the possibility of universal quantum computing, creating the corresponding experiments include their own issues. One of them is the application of two-qubit gates in non-neighboring components. How could it be possible to apply a two-qubit gate in non-neighboring components if they cannot interact directly with each other? The answer lies in quantum gate teleportation.

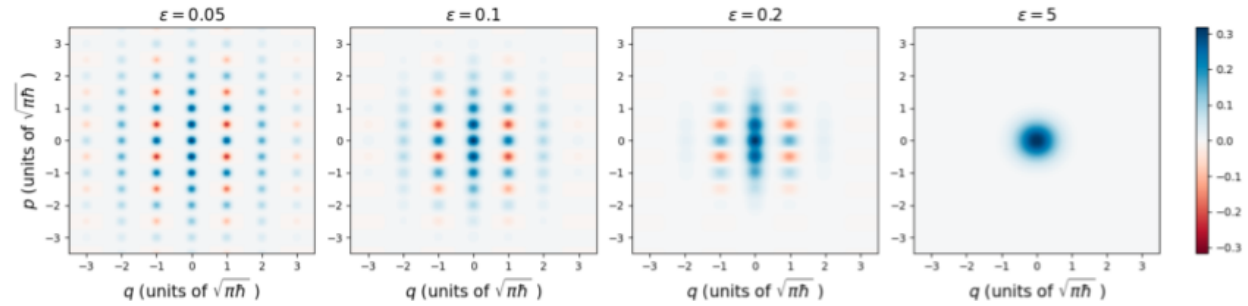

Figure 8: Finite energy GKP States

Quantum gate teleportation is analogous to quantum state teleportation. In quantum state teleportation, a quantum state is sent from one location to another. In quantum gate teleportation, a quantum gate is effectively applied with two-distant sources. They both require shared entanglement between both locations as well as classical communication channels, but serve different purposes.

3 Experimental Background

3.1 CNOT Gate Between Non-Neighboring Modes via Gate Teleportation: Architecture

A recent experiment demonstrated a deterministic teleported form of the CNOT gate[1]. The architecture of the experimental setting is shown in Fig. 9. This modular architecture is characterized by nodes and communication channels connecting them, which can be turned on or off. Each node contains data qubits and communication qubits encoded in cavity modes and transmon modes, respectively. The transmon modes are connected to readout resonators. The communication channels are implemented using bus modes. This architecture is relevant because of its scalability advantage; meaning the possibility of creating more qubits that also work efficiently as well as quantum gates that can act on them. However, to have universal quantum computation with this architecture, it will be necessary to implement two-qubit gates between data qubits. Notice that the data qubits are non-neighboring, so an alternative method will be required.

3.2 CNOT Gate Between Non-Neighboring Modes via Gate Teleportation: Teleportation Circuit

As mentioned in Section 2.6, it is possible to implement a two-qubit gate between two distant modes using gate teleportation. Fig.9 shows the teleported circuit architecture for a CNOT gate between two data qubits in the architecture

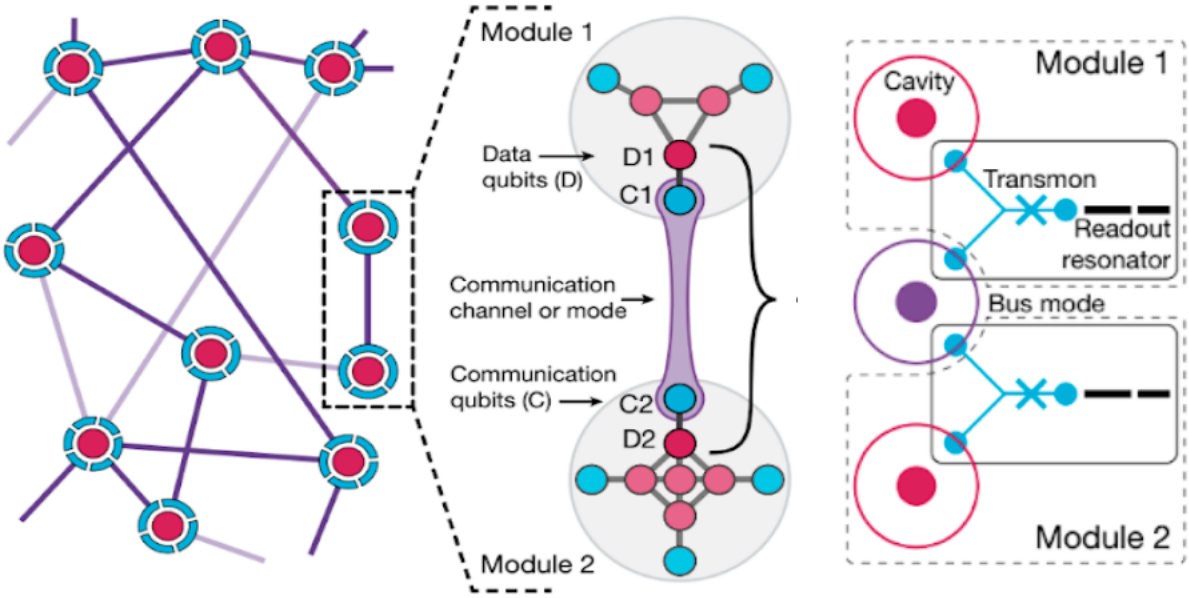

Figure 9: Module architecture used to implement a teleported CNOT gate. Image taken from reference 1.

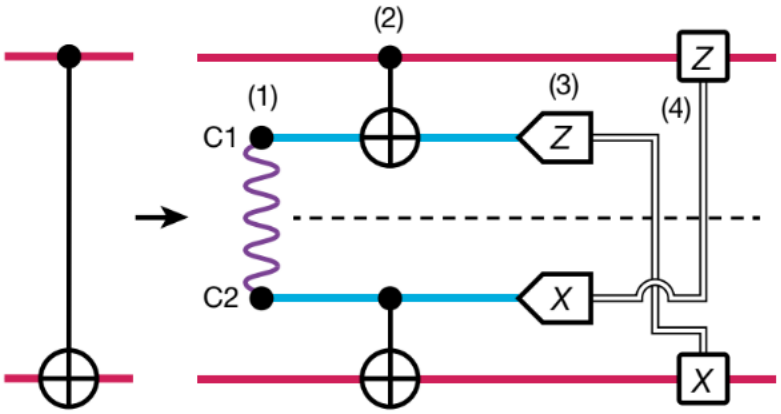

Figure 10: CNOT gate and its teleported form between two data qubits. Image taken from reference 1.

just presented. Part (1) denotes entanglement between communication qubits C1 and C2, part (2) denotes a local CNOT gate between each pair of a data and communication qubits, part (3) represent Pauli Z and X measurements. Part (4) represents classical communication channels that the measurement results as parameters to conditional Z and X gates.

This circuit was achieved experimentally with a process fidelity of 79% when the binomial code, defined below, was used in the data qubits

$$\begin{aligned} |0\rangle_L &= |2\rangle \\ |1\rangle_L &= \frac{|0\rangle + |4\rangle}{\sqrt{2}}. \end{aligned} \tag{10}$$

Here, the subscript L denotes a logical qubit state. This error was used because it allows for the detection of photon loss, a common error type in this architecture.

3.3 Objective: Teleported CNOT Gate between GKP States

Now that a teleported CNOT gate experiment has been introduced with the binomial code, we can ask if the same thing can be done with other types of qubit encoding for the data qubits. In particular, what if the encoding used is based on GKP states?

In order to do so, we would first need a continuous variable version of the CNOT gate as well as a teleportation form of that gate.

4 Simulation Background

4.1 Continuous Variable Version of Teleported CNOT Gate

The continuous variable version of a CNOT gate is called the CX (Controlled-X) (or SUM, or QND) gate. It is labelled in this report as $CX(s)$, where s is the gate's parameter such its action on states represented in position space look as

$$CX(s)\left|x_1, x_2\right\rangle_s = \left|x_1, x_2 + s x_1\right\rangle. \tag{11}$$

Here, 1 and 2 would represent the control and target modes, respectively. In the Heisenberg picture, the $CX(s)$ operator transforms the quadrature operators as follows

$$\begin{aligned} CX(s)^\dagger \hat{x}_1 CX(s) &= \hat{x}_1 \\ CX(s)^\dagger \hat{p}_1 CX(s) &= \hat{p}_1 - s\hat{p}_2 \\ CX(s)^\dagger \hat{x}_2 CX(s) &= \hat{x}_2 + s\hat{x}_1 \\ CX(s)^\dagger \hat{p}_2 CX(s) &= \hat{p}_2. \end{aligned} \tag{12}$$

Is there a teleported version of the $CX(s)$ gate? The answer is yes. The corresponding teleported circuit is presented in Fig. 11. In this circuit, modes 1 and 2 are entangled and used with modes A and B for local $CX(s)$ gates. Homodyne measurments are then done on modes 1 and 2, and that information is transferred via classical communication channels as parameters for displacement gates on modes A and B. This circuit yields the following output state in the Heisenberg representation

$$\begin{aligned} \hat{x}'_A &= \hat{x}_A \\ \hat{p}'_A &= \hat{p}_A - g^2\hat{p}_B - g(\hat{p}_1 - \hat{p}_2) \\ \hat{x}'_B &= \hat{p}_B + g^2\hat{x}_A + g(\hat{x}_1 + \hat{x}_2) \\ \hat{p}'_B &= \hat{p}_B. \end{aligned} \tag{13}$$

If we ignore for a moment the last terms in the middle equations, we can see that this circuits effectively produces a $CX(s)$ gate with a parameter of $s = g^2$, where g is the parameter used in the local QND gates of the teleported circuit. So if we want to effectively create such gate every time, we have to guarantee that the last terms in the middle equations are effectively zero.

4.2 Objective: Find Two-Mode Squeezing Gate Parameter That Produces an Effective CNOT Gate Between GKP States

There are two requirements to effectively implement an ideal $CX(s)$ gate using its teleported form. The first one is entanglement between modes 1 and 2. The

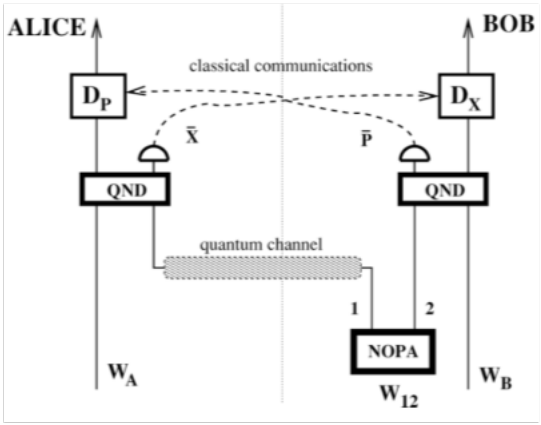

Figure 11: Teleportation circuit that implements a $CX(s)$ gate. Image taken from reference 3.

second one is a having a value of effectively zero in the terms of $g(\hat{p}_1 - \hat{p}_2)$ and $g(\hat{x}_1 + \hat{x}_2)$. An important note to make is that throughout this study, only the case $g = 1$ was considered. This means only the case where the teleported circuit approaches an ideal $CX(s)$ gate with parameter $s = g^2 = 1$ was considered. So really, we are looking to design a circuit such that the terms $(\hat{p}_1 - \hat{p}_2)$ and $(\hat{x}_1 + \hat{x}_2)$ are effectively zero.

The entanglement requirement between modes 1 and 2 can be achieved using a two-mode squeezing gate. As noted earlier, this gate creates correlations between the position operators and anticorrelations in the momentum operators. Recall that this gate is parametrized by a parameter r. Under the action of this gate, the expectation values of individual position and momentum operators $\hat{x}_i$ and $\hat{p}_i$ for $i \in \{1, 2\}$ are zero since the two-mode squeezing gate does not change the vector of means of these states. But even if the expectation values are zero, we would also like the variances to be zero since that will guarantee that the variables $(\hat{p}_1 - \hat{p}_2)$ and $(\hat{x}_1 + \hat{x}_2)$ are effectively zero.

Recall that variances in linear combinations of the operators $\hat{x}_i$ and $\hat{p}_i$ for $i \in \{1, 2\}$ will be squeezed under the action of a two-mode squeezing gate, as shown in Eqs. . Looking at those equations, we can see that a negative value of r will decrease the values of $(\hat{p}_1 - \hat{p}_2)$ and $(\hat{x}_1 + \hat{x}_2)$ So the objective now is to find a parameter for the two-mode squeezing gate such that the variance in these variables is low enough.

5 Numerical Simulations

Now that the main task to complete has been layed out, results from a few simulations are presented in search of the two-mode squeezing gate that satisfies the requirements already mentioned.

5.1 First Simulation: Fidelity Between CX and Teleported CX Circuits for GKP States

To find a reliable value of the two-mode squeezing parameter, fidelity was used to compare the output states of the CX circuit and its teleported form. Fidelity is a measure of the closeness of two quantum states; a value of 1 in fidelity means that two states are identical, while a value of 0 means that the states are orthogonal. For two quantum states described by the density matrices σ and ρ, the fidelity $F(\sigma, \rho)$ can be computed as

$$F(\sigma, \rho) = (\mathrm{tr}\sqrt{\sqrt{\rho}\sigma\sqrt{\rho}})^2. \tag{14}$$

The question now is, what states should be used as the input states in both circuits during this test? We can use the input states of a CNOT truth table with a GKP state encoding. The CNOT truth table is presented in Fig. 888. This would not only tell us that the two circuits yield the same output when GKP states are used but also help us construct a CNOT truth table and therefore verify that the teleported circuit indeed yields an effective CNOT gate when a GKP encodings for the control and target modes are used. Figs. 13 - 16 show plots of the logarithm base 10 of 1-fidelity between the CX circuit and its teleported version as functions of the two-mode squeezing gate parameter used for input states with GKP encoding based on the input states of a CNOT truth table.

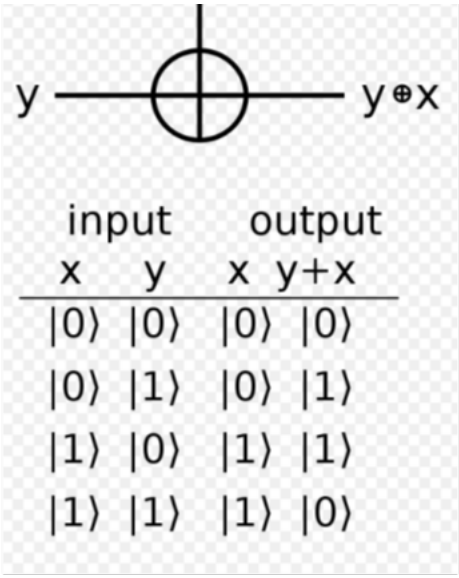

Figure 12: CNOT truth table. Image taken from Wikipedia.

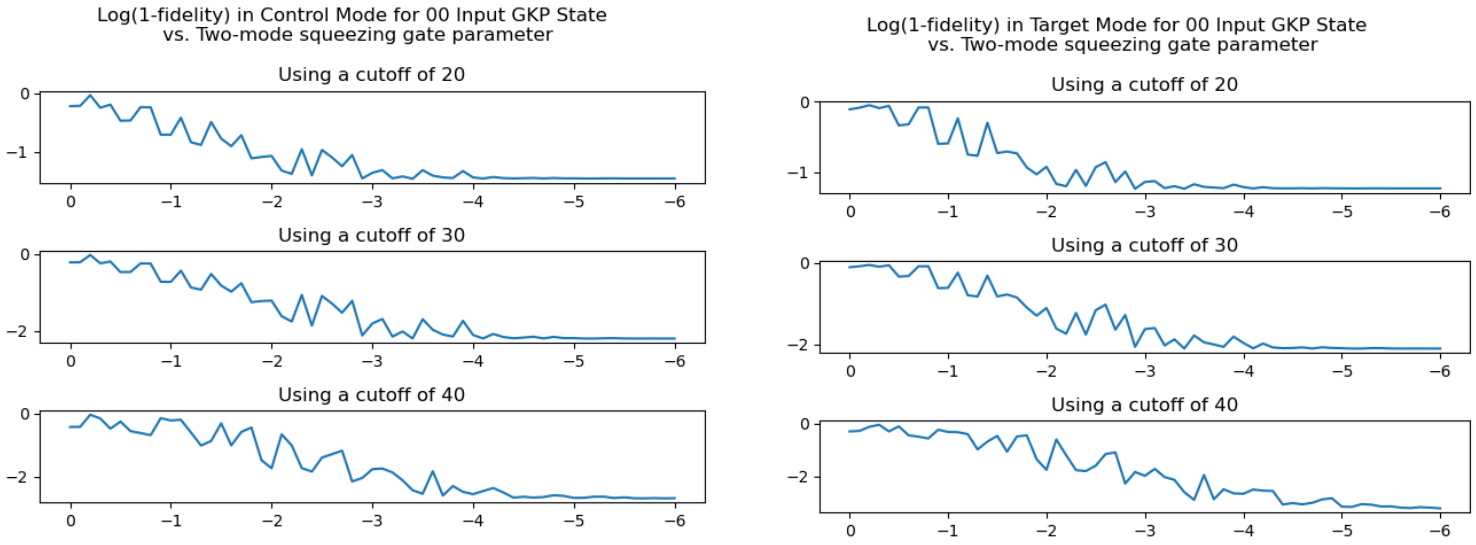

Figure 13: Log(1-fidelity) for Input state $|0\rangle_{GKP}|0\rangle_{GKP}$ as functions of the two-mode squeezing gate parameter r

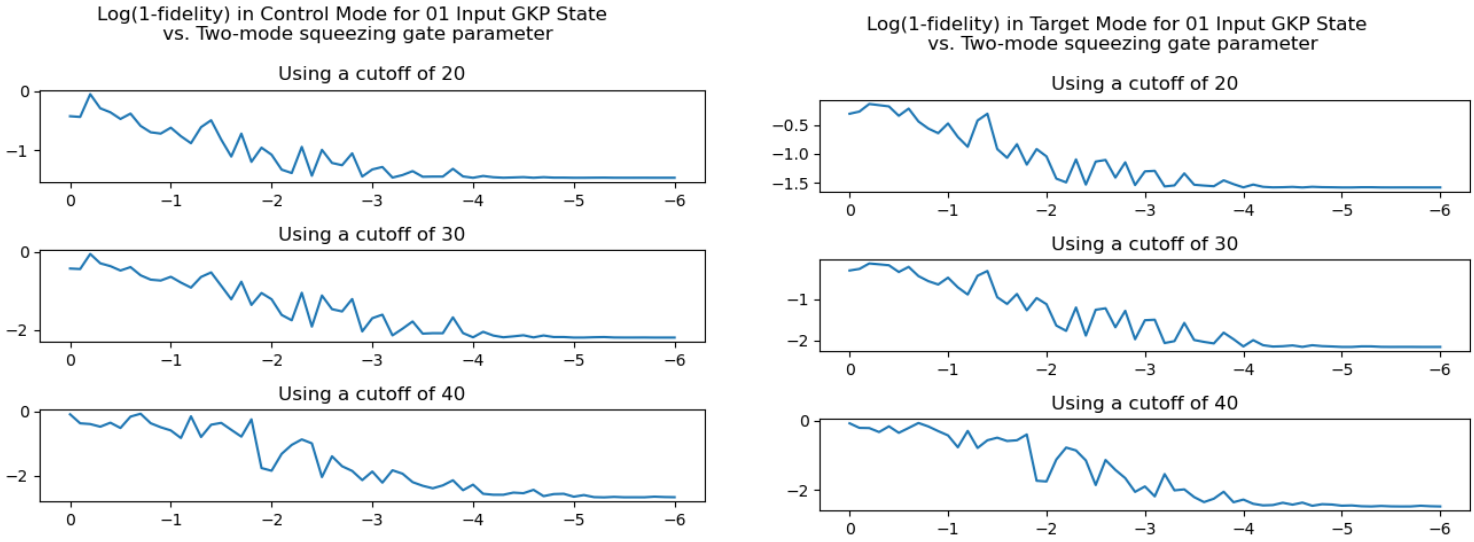

Figure 14: Log(1-fidelity) for Input state $|0\rangle_{GKP}|1\rangle_{GKP}$ as functions of the two-mode squeezing gate parameter r

Figure 15: Log(1-fidelity) for Input state $|1\rangle_{GKP}|0\rangle_{GKP}$ as functions of the two-mode squeezing gate parameter r

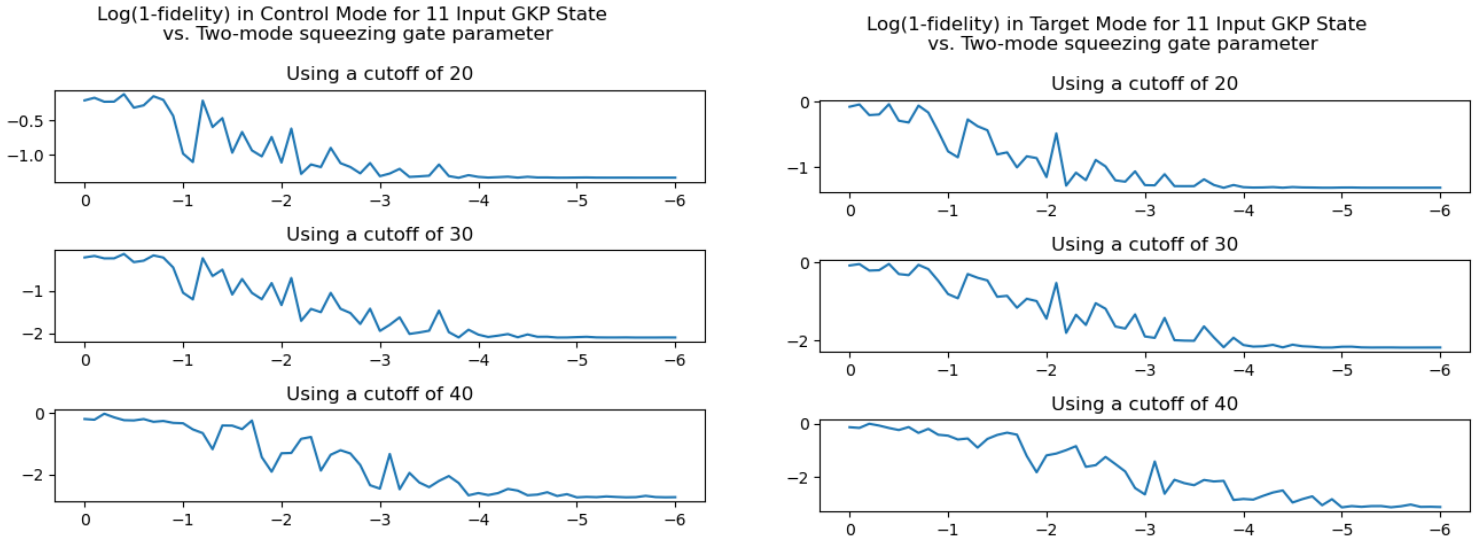

Figure 16: Log(1-fidelity) for Input state $|1\rangle_{GKP}|1\rangle_{GKP}$ as functions of the two-mode squeezing gate parameter r

5.1.1 Second Simulation: CNOT Truth Table

Even if the fidelity between both circuits is of 99%, how can we guarantee that a CNOT is effectively implemented? In other words, how can we guarantee that a $CX(s)$ gate effectively yields a CNOT gate when GKP states are used? We can look at the output Wigner functions to do so. By looking at the output Wigner functions, we can identify the output states to be $|0\rangle_{GKP}$ or $|1\rangle_{GKP}$. Figs. 888 through 888 show the output Wigner functions when GKP input states corresponding to input states of a CNOT truth table are used. All input GKP states used in these simulations had a damping parameter of $\epsilon = 0.15$.

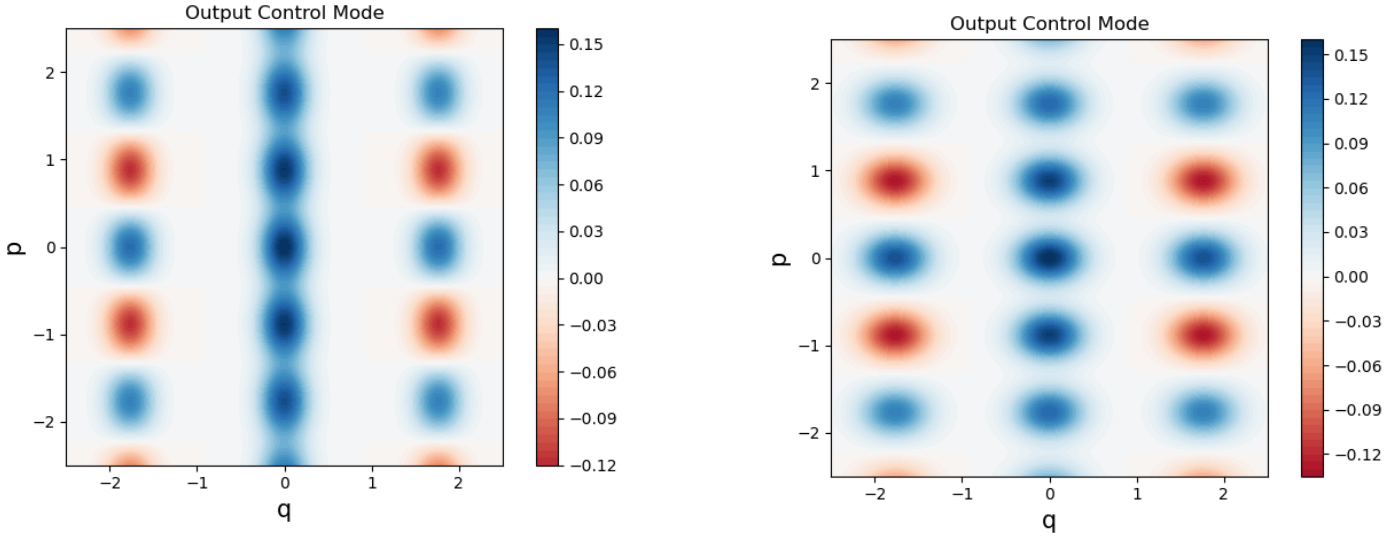

Figure 17: Output Wigner functions of the control mode(left) and target mode (right) for the case where its input state is $|0\rangle_{GKP}|0\rangle_{GKP}$

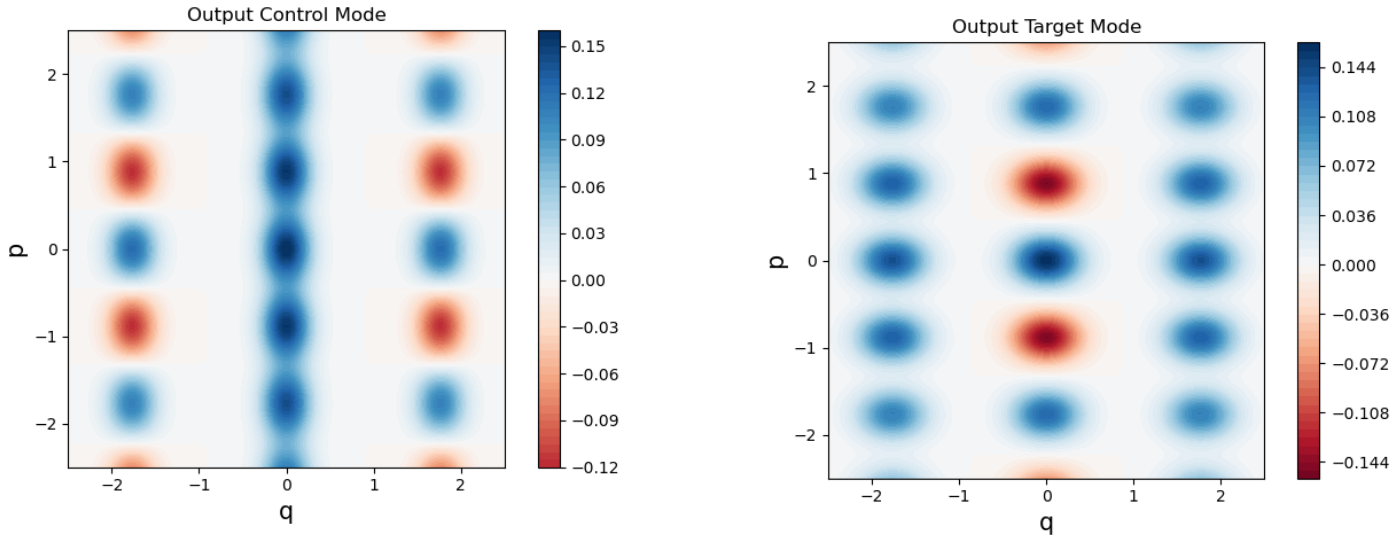

Figure 18: Output Wigner functions of the control mode(left) and target mode (right) for the case where its input state is $|0\rangle_{GKP}|1\rangle_{GKP}$

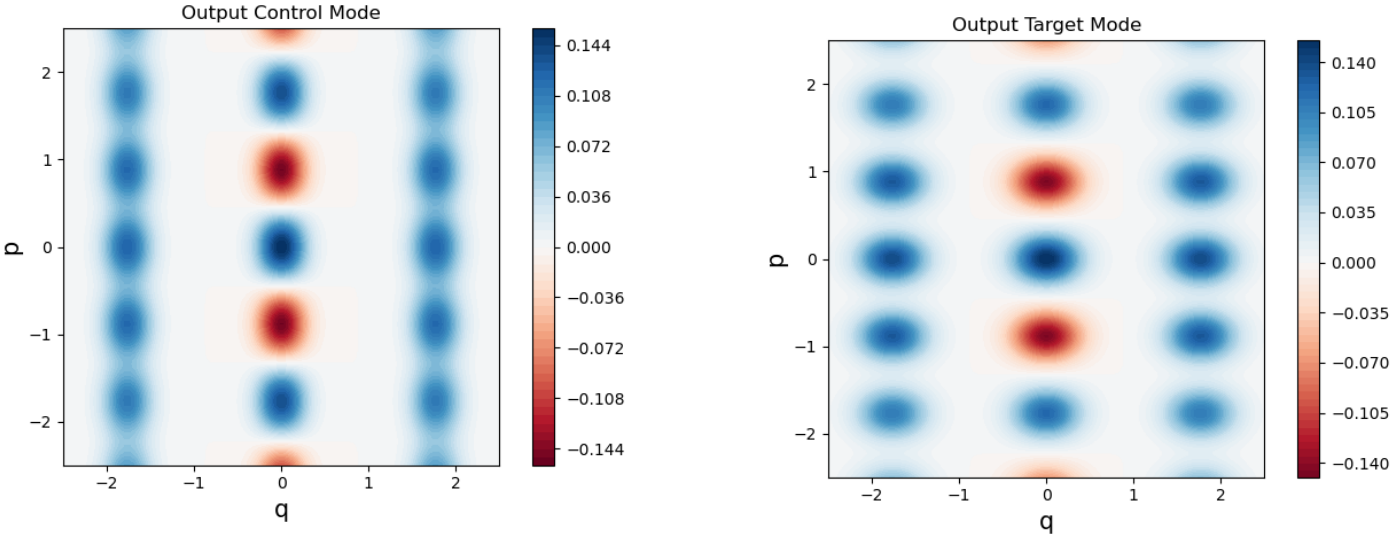

Figure 19: Output Wigner functions of the control mode(left) and target mode (right) for the case where its input state is $|1\rangle_{GKP}|0\rangle_{GKP}$

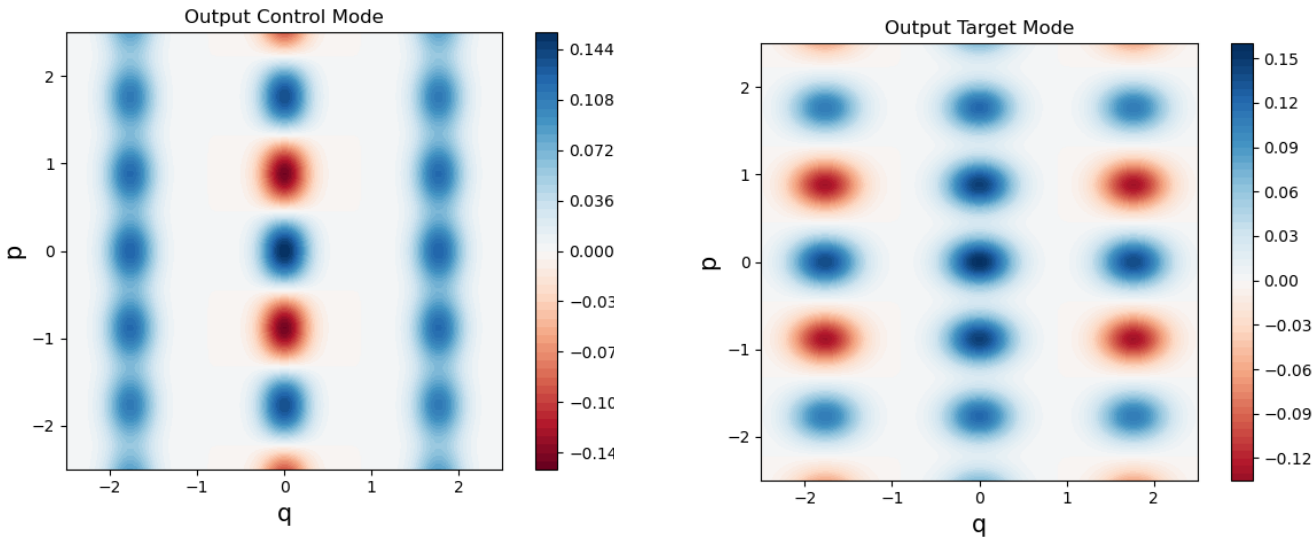

Figure 20: Output Wigner functions of the control mode(left) and target mode (right) for the case where its input state is $|1\rangle_{GKP}\,|1\rangle_{GKP}$

5.2 Third Simulation: Fidelity Between CX and Teleported CX Circuits for GKP States with Amplitude Damping

Another simulation of fidelity was done with amplitude damping incorporated. Amplitude damping is a quantum channel that models a common type of experimental error in the superconducting model of quantum computing. This channel couples the lowering operator $\hat{a}$ of a mode to the lowering operator $\hat{b}$ of the vacuum state representing the environment as follows

$$\hat{a} \mapsto \sqrt{T}\hat{a} + \sqrt{1-T}\hat{b}, \tag{15}$$

where $0 \geq T \leq 1$ is the loss parameter. A value of $T = 1$ represents no coupling to the environment, while a value of $T = 0$ represents full coupling to the environment. For the simulated circuit, loss channels with the following values were used

- $T = 0.95$ for the control and target modes.
- $T = 0.9$ for the entangled modes after the two-mode squeezing gate and before the local QND gates.
- $T = 0.6$ for the entangled modes after the local QND gates and before their measurments.

Plots of log(1-fidelity) were obtained again for the control and target modes. These are shown in Figs. 21-24.

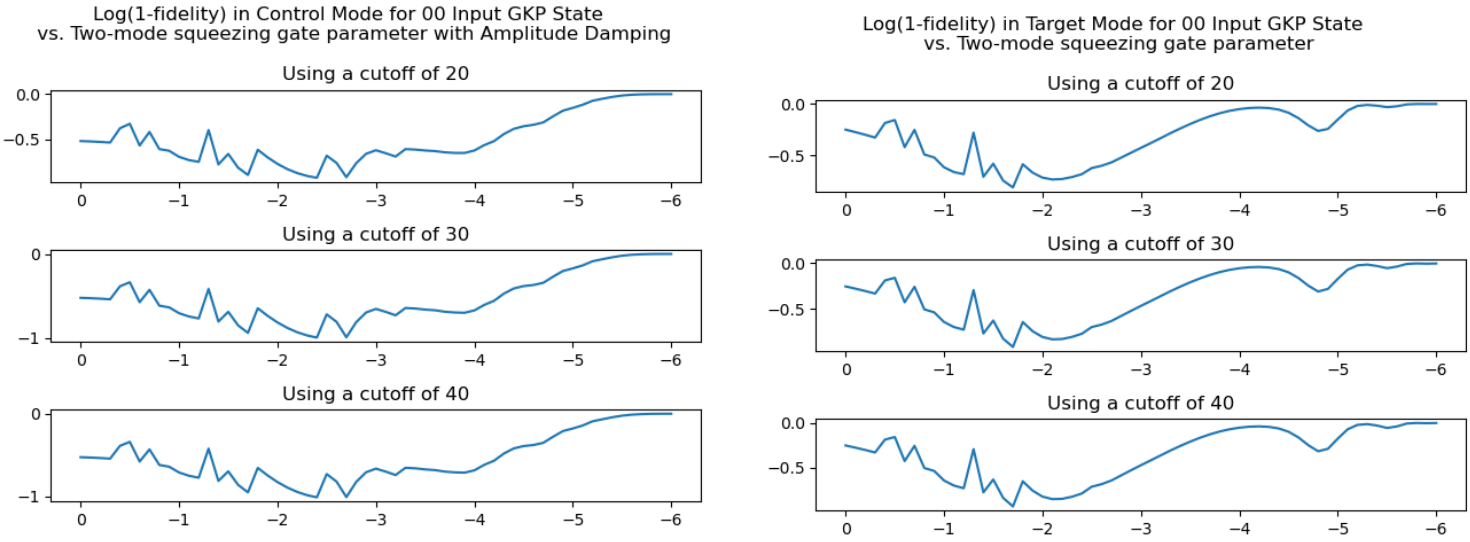

Figure 21: Log(1-fidelity) for Input state $|0\rangle_{GKP}|0\rangle_{GKP}$ as functions of the two-mode squeezing gate parameter r with amplitude damping incorporated

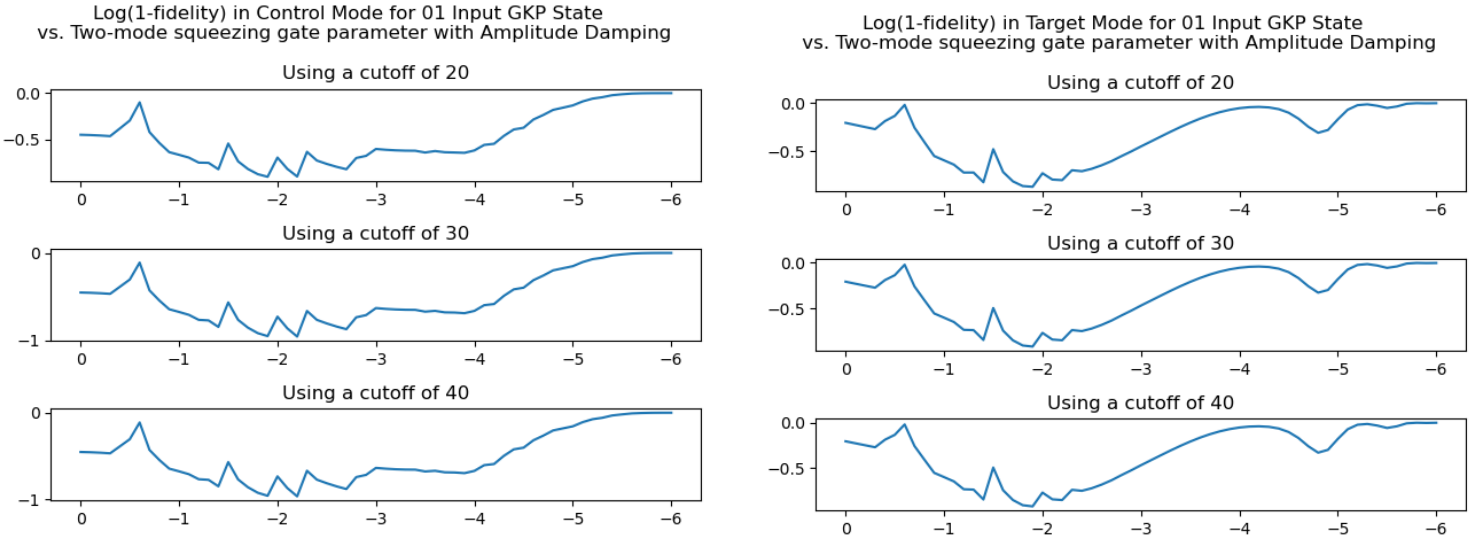

Figure 22: Log(1-fidelity) for Input state $|0\rangle_{GKP}|1\rangle_{GKP}$ as functions of the two-mode squeezing gate parameter r with amplitude damping incorporated

Figure 23: Log(1-fidelity) for Input state $|1\rangle_{GKP}|0\rangle_{GKP}$ as functions of the two-mode squeezing gate parameter r with amplitude damping incorporated

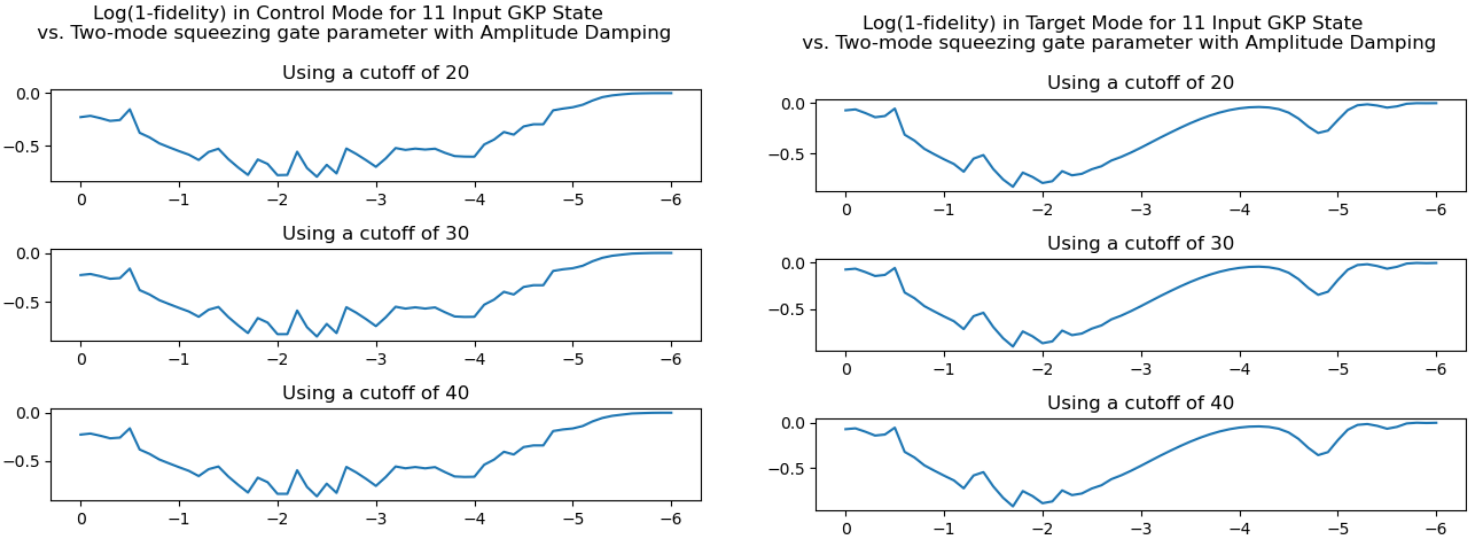

Figure 24: Log(1-fidelity) for Input state $|1\rangle_{GKP}|1\rangle_{GKP}$ as functions of the two-mode squeezing gate parameter r with amplitude damping incorporated

5.3 Fourth Simulation: Variances in Shared Entangled State as Functions of the Parameter

Another simulation was done in search of a parameter that would give low variance in the variables $(\hat{p}_1 - \hat{p}_2)$ and $(\hat{x}_1 + \hat{x}_2)$ of the teleported CX circuit. This consists of running a circuit with two vacuum states acted upon by a two-mode squeezing gate, and plotting the variance as a function of the parameter used in the two-mode squeezing gate. This simulation had to be done using the Fock backend from Strawberry Fields because the analytic expression of the variances included a term that could not be evaluated using other backends. Using the Fock backend means representing quantum states using the Fock basis, which meant large amounts of time to run the simulations. The Fock backend used is also determined by a cutoff, the largest number state used in the representation of the quantum state. So multiple simulations were done using different choices of the cutoff. Figs. 25 to 27 show the corresponding simulations for cutoffs of 20,30, and 40. The variance in the opposite variables $(\hat{p}_1 + \hat{p}_2)$ and $(\hat{x}_1 - \hat{x}_2)$ was also plotted to have a test-check; if the variance of $(\hat{p}_1 - \hat{p}_2)$ and $(\hat{x}_1 + \hat{x}_2)$ decreases, then the variance of $(\hat{p}_1 + \hat{p}_2)$ and $(\hat{x}_1 - \hat{x}_2)$ should increase. This behavior is correctly noted at the beginning of each plot for each choice of a cutoff. However, there is an inflection point with appears at a later value of the parameter if the cutoff is increased. This inflection point is not expected, and does not allow us to determine a value of the parameter that yields a low enough variance in $(\hat{p}_1 - \hat{p}_2)$ and $(\hat{x}_1 + \hat{x}_2)$. That is why these plots were not considered as a reliable method to find the two-mode squeezing gate parameter value.

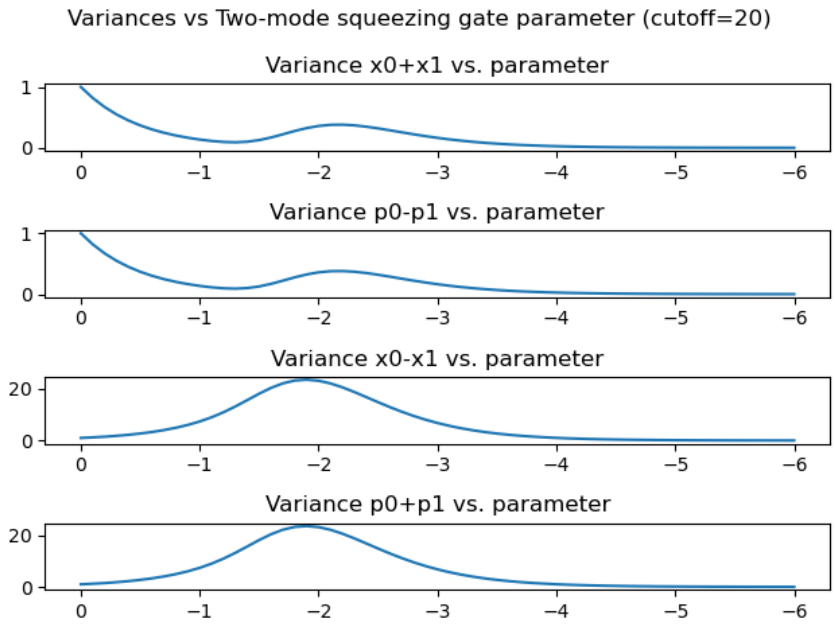

Figure 25: Variances for a cutoff of 20

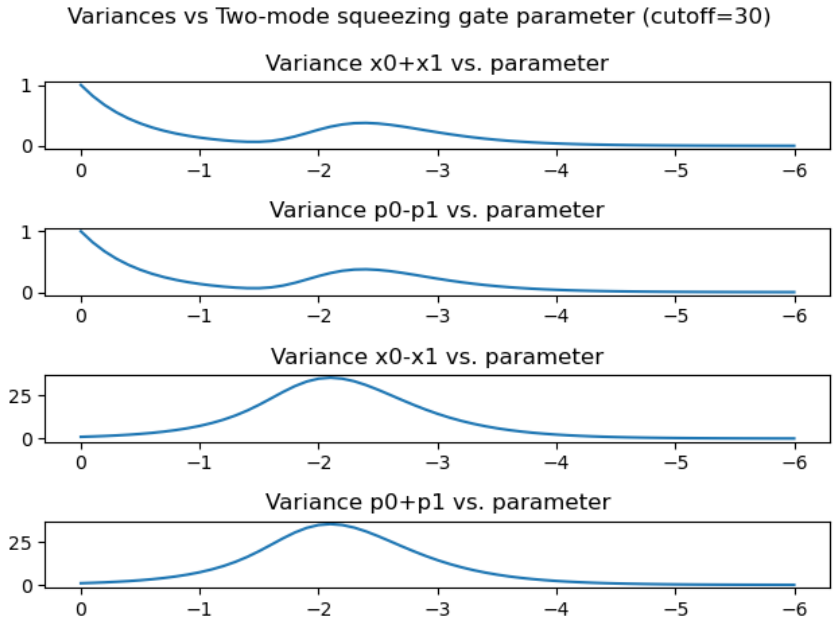

Figure 26: Variances for a cutoff of 30

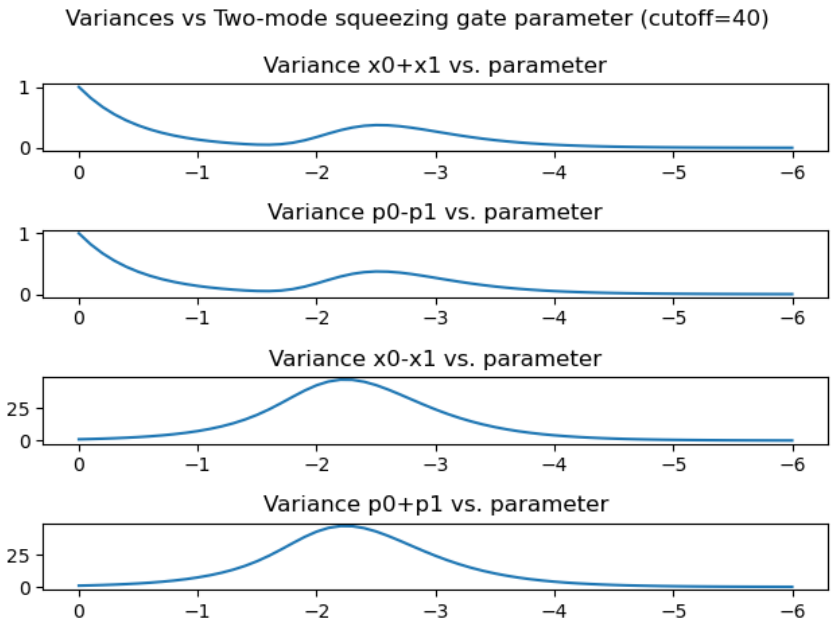

Figure 27: Variances for a cutoff of 40

6 Further Directions

This study has several directions to be extended. The first extension is a reasoning of the behavior shown in the variance plots from the last section. In particular, it has to be understood why the inflection point changes for different choices of the cutoff and it there is a cutoff that would yield a reliable value of the parameter. Alternatively, a different library such as QuTip could be used to obtain the same plots without the need of representing the state in the Fock basis.
Another extension is to incorporate other types of error in the circuit. These errors could include phase damping and/or measurement errors. From here, new fidelity plots can be obtained.
This study only considered the case where the teleported CX circuit approaches an ideal CX circuit of parameter $s = 1$. Other cases could be considered. In particular, it is possible that other choices of this parameter yield better fidelities under the influence of the error types just mentioned.
Lastly, it is important to note that all simulations shown here involved using GKP states with a damping parameter of $\epsilon = 0.15$. Other choices of this parameter could also give better fidelities under the influence of error.

7 Skills Learned

Several skills were learned throughout this project. The first skill involved understanding new theory on quantum optics. This meant getting familiar with the continuous variable form of quantum computing. Another skill developed was using online libraries to simulate quantum circuits. This involved understanding an API and implementing it. Within this process, new programming techniques had to be learned to implement these programs efficiently. Another skill developed consists of presentation. The progress in this project had to be communicated almost weekly, so the numerical results had to be presented efficiently with the use of plots, identification of issues, and questioning of further directions.

8 References

1. Chou, K.S., Blumoff, J.Z., Wang, C.S. et al. Deterministic teleportation of a quantum gate between two logical qubits. Nature 561, 368–373 (2018). https://doi.org/10.1038/s41586-018-0470-y

2. Nathan Killoran, Josh Izaac, Nicol as Quesada, Ville Bergholm, Matthew Amy, and Christian Weedbrook. "Strawberry Fields: A Software Platform for Photonic Quantum Computing", Quantum, 3, 129 (2019).

3. Filip, Radim. "Continuous-variable quantum nondemolishing interaction at a distance." Physical Review A 69 (2004): 052313.

4. Campagne-Ibarcq, P., Eickbusch, A., Touzard, S. et al. Quantum error correction of a qubit encoded in grid states of an oscillator. Nature 584, 368–372 (2020). https://doi.org/10.1038/s41586-020-2603-3

5. Loudon, Rodney, and Peter L. Knight. "Squeezed light." Journal of modern optics 34.6-7 (1987): 709-759.